MEASURING ANISOTROPY IN MICROWAVE SUBSTRATES

Murray Olyphant, Jr.
3M Co., Electronic Products Laboratory
St. Paul, Minnesota 55101

ABSTRACT

A split TE_{111} cavity is described which enables the accurate measurement of the within-plane dielectric constant of a 1 inch disk cut from substrates in the range 25 to 125 mils in thickness. HP 67/97 programs are included for both end and center located specimens.

Introduction

Optimization of microwave circuit design requires that anisotropy in dielectric substrates be taken into account. Many widely used microwave dielectrics exhibit significantly higher dielectric constant within the plane of the substrate than normal to it. When properly provided for, a higher ϵ_r in the substrate plane can reduce the difference between odd and even mode velocities in microstrip and provide improved coupler and filter performance[1,2]. The properties of microstrip lines on anisotropic substrates have been derived using Green's functions or other techniques[1,3,4,5,6]. Szentkuti has offered a transformation to an electrostatically equivalent isotropic substrate geometry[2,7].

Design methods for anisotropic substrates are of little use without an accurate knowledge of dielectric constant along the three substrate axis identified in Figure 1. In this paper the z axes is chosen normal to the substrate surface because this orientation

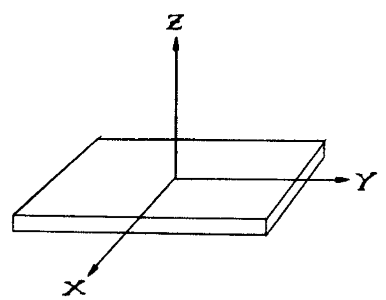

Figure 1: Substrate axes for anisotropy measurements

coincides with the axis of the cylindrical cavities used for measurements. Thus the x-y plane parallels the substrate surface. The z-direction dielectric constant, ϵ_z is relatively easy to measure. Simple, accurate methods for testing actual substrates (as opposed to specially prepared samples) are available[8-14]. In contrast, the x-y plane value(s) ϵ_{xy}, are much more difficult to determine on thin sheets. Anisotropy is often a function of the substrate fabrication process and so may vary with substrate thickness. Thus conventional waveguide and co-axial line measurements, which require thick specimens, are unreliable.

This paper describes a simple and usefully accurate method for measuring the x-y dielectric constant of unmetallized 1 inch disks machined from a single layer of substrates in the range 10 to 125 mils in thickness. This test complements a previously reported method for determining ϵ_z using a completely metallized disk[10,13]. Both tests may be run on the same specimen. Comparison of the two methods is helpful.

Useful TM and TE Modes

Those resonant modes in right circular cylindrical cavities which are of interest here are identified in the chart of Figure 2. In $TM_{n\ell 0}$ modes the electric

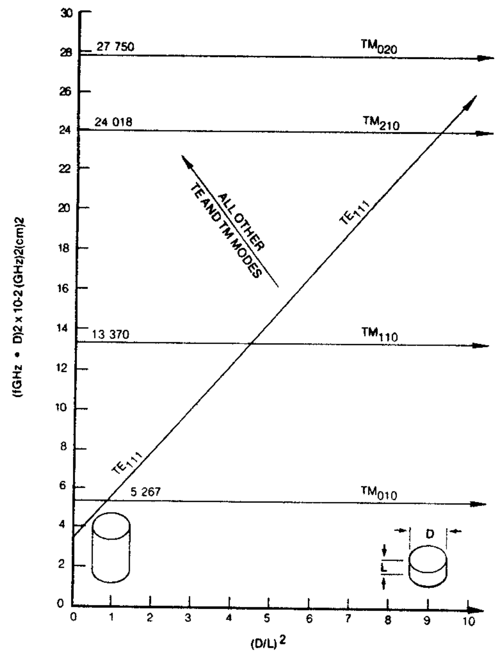

Figure 2: Mode chart for right circular cylinders showing the relationship of $TM_{n\ell 0}$ and TE_{111} modes.

field has only a z (axial) component. In a cavity resonant in the TE_{111} mode the E-field has no z component. All TE field lines lie in planes perpendicular to the axis. Their major component is parallel to a particular diameter determined by cavity excitation.

In cavities made by plating dielectric disks for which the ratio of thickness to diameter is less than 0.128 at least the first 17 resonant modes are all $TM_{n\ell 0}$. In these modes the electric field is perpendicular to the disk faces and the resonant frequency is independent of cavity height (i.e. of substrate thickness). Only the diameter needs to be accurately known. Dielectric constant is equal to the square of the ratio of empty (calculated) to filled cavity resonant frequency for the same modes. Accuracy is typically 0.1 to 0.2%.

In order to impress a TE field edgewise through a dielectric disk it must be tested unmetallized in an axially much longer cavity. The cavity length is preferably sufficient to lower the desired TE_{111} resonance (the lowest frequency TE mode) below the TM_{010} mode (i.e. $L > D$).

Experimental

The split cavity developed for measurement of ϵ_{xy} is shown disassembled in Figure 3. The inside diameter

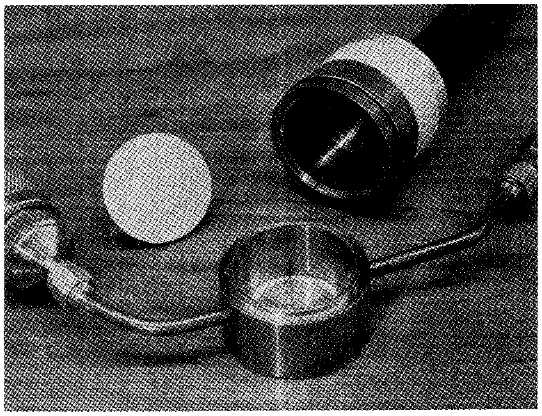

Figure 3: TE_{111} cavity shown disassembled. Specimen (upper left) is pressed against top of cavity (upper right) by vacuum and can be turned through TE field established by probes in lower half of cavity.

is 2.540 cm and the inside length when assembled approximately 2.94 cm. Test specimens may be either pressed into intimate contact with the upper end by vacuum applied through small holes or, for greater sensitivity in the case of the thinnest disks, located at the center. Potential inaccuracies are large for thin specimens located at the end of the cavity, principally because of the rapidly changing E-field near the short and consequent sensitivity to any air gap between specimen and cavity wall. It has been found that the conformability of Teflon* based materials (which are of particular interest) allows them to be pressed by vacuum into generally acceptable contact with the end wall.

End Located Specimens

Figure 4 diagrams the significant features of the cavity with the specimen at one end. In this case the condition for resonance, neglecting losses, is $Z_1 = -Z_2$. This equation becomes, in terms of wave impedance and dimensions

$$Z_d \tan(2\pi t/\lambda_{gd}) = -Z_o \tan 2\pi(L-t)/\lambda_{go} \qquad (1)$$

*Registered trademark, E.I. DuPont Co.

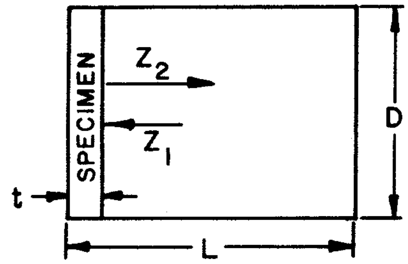

Figure 4. Cavity parameters

where Z_d and Z_o are the guide wave impedances in the dielectric and empty cavity respectively, and λ_{gd} and λ_{go} are the guide wavelengths in the dielectric and empty guide. The general expression for guide wave impedance[15], $Z = \eta(1-(f_o/f)^2)^{-1/2}$ becomes for the TE_{111} mode, $Z = \eta_o(\epsilon_r - (\lambda_o/3.413a)^2)^{-1/2}$ where η_o is the wave impedance in free space, λ_o is free space wavelength and $a = D/2$. The guide wavelength $\lambda_g = \lambda(1 - (f_c/f)^2)^{-1/2}$ similarly becomes for the TE_{111} case $\lambda_g = \lambda_o(\epsilon_r - (\lambda_o/3.413a)^2)^{-1/2}$. When these substitutions are made in Equation 1 and the expressions for $(\lambda_o/3.413A)^2$ and $2\pi/\lambda_o$ are simplified for $a = 1.270$ cm to $47.84/(f_{GHz})^2$ and $0.2096\, f_{GHz}$ respectively the equation for TE_{111} resonance in a 2.540 cm diameter cavity becomes

$$(\tan X_1)/X_1 = -[(L-t)/t]\,(\tan X_2)/X_2 = Y \qquad (2)$$

in which

$$X_1 = 0.2096t\,[\epsilon_{XY} f^2 - 47.84]^{1/2} \qquad (2a)$$

$$X_2 = 0.2096\,(L-t)[f^2 - 47.84]^{1/2} \qquad (2b)$$

The HP 67/97 program listed at the end of the paper first calculates the value, Y, of the right hand side of Equation 2 using 2b. The value of $(1-1/Y)$ is stored as a reference for successively correcting the estimated X_1 until the correction is 1.0000. The program pauses to display successive corrections. This algorithm is addressed by Label B. Once X_1 is known Label E solves equation (2a) for ϵ_{XY}.

Center Located Specimens

When the specimen is located centrally along the axis we make the assumption that resonance occurs for a quarter wave shorted cavity with an open circuit in the center of the specimen. In the program the first pause after the calculation of L allows inserting a subroutine Label C, to reduce the values of L and t by one half before continuing the calculation of Y as above. Since for a center located specimen Z_1 looks through half the specimen into an open circuit Eq. 2 becomes

$$1/X_1 \tan X_1 = Y \qquad (3)$$

and a new algorithm is required to find X_1. The program returns control to the keyboard after calculating Y to allow selection of the proper subroutine. The center specimen Label D subroutine first calculates a new reference $(Y + 1/3)$ to which values of $[(1/X_1 \tan X_1) + 1/3]$ calculated for successive estimates of X_1, are compared to generate corrections to the estimate. The iteration stops when the correction (displayed during Pause) is 1.0000. In some repeatable circumstances associated with center specimen calculations the author's HP 67 will not perform the required fractioning in step 133 and so stays in the correction loop mode. In this case the subroutine to calculate ϵ_r is manually selected by pressing R/S and E during any pause displaying 1.0000.

TABLE I

DATA FOR DIELECTRIC ANISOTROPY

Line	Material	Designation/ Description	Thick Mils	Loc.	7.5 - 9.5 GHz ϵ_z	ϵ_{xy}	%XY Anisot.	ϵ_{xy}/ϵ_z
1	Teflon	Disk cut from						
2		rod						
3		#1	102.8	E	2.08	2.11	Neg	--
4		#2	102.6	E	2.08	2.12	Neg	--
5		both	205.4	E	2.08	2.09	Neg	1.005?
6		#2	102.6	C	2.08	2.08	Neg	
7	TFE/glass	CuClad 217	2x10.0	C	2.15	2.34	Neg	1.09
8	cloth	Old GX 245	60	E	2.45	2.95		
9						2.89	2.0	1.19
10		New GX 245						
11		#1	60.3	E	2.43	2.87	Neg	
12		#2	60.2	E	2.43	2.88	Neg	
13		both	102.5	E	2.43	2.81	Neg	1.16
14		#1	60.3	C	2.43	2.78	Neg	
15		#2	60.3	C	2.43	2.78	Neg	
16	Loaded TFE/							
17	Glass Cloth	CL 606						
18		#1	60.6	E	6.24	6.64		
19						6.56	1.2	1.06
20		#2	59.9	E	6.09	6.64		
21						6.61	.45	1.08
22								
23	Loaded					9.15		
	Styrene	CHK9	102.5	E	9.12	8.89	2.9	1.01

Results and Discussion

Values of both ϵ_z and ϵ_{xy} are given in Table 1 for typical commercial materials with dielectric constants ranging from 2.08 to 9.1. The fourth column gives the disk thickness, or the sum of two disks when two are tested together. In the later case a small hole was drilled in the center of the disk against the wall to apply vacuum to the second disk. In the fifth column E indicates a specimen tested at the end of the cavity; C shows central positioning. The ϵ_z measurements were made on plated disks. Where there are several values of ϵ_{xy} reported for a material the underlined value is the one believed to be most accurate. When two values are given for one disk these are the minimum and maximum observed by rotating the cavity top. The comment "neg" means the difference between maximum and minimum ϵ_{xy} was less than 0.33% which is within experimental error. It was not possible to position a single disk of 10 mil CuClad 217 (Line 8) in the center of the cavity so two were adhered with a very light film of oil. The result agrees well with thicker specimens of this material. Because of slightly non-square glass weave, the old GX-060-45 construction did exhibit a within plane anisotropy of about 2%. A new construction has reduced this anisotropy to a negligible level. The data for the loaded TFE coated cloth indicate that the attempt to make this product isotropic by raising the dielectric constant of the coating up to the glass has been only partly successful. Even though the loaded styrene material was cast and might be expected to exhibit negligible anisotropy the TE_{111} cavity reveals considerable variation of ϵ_{xy} around the axis. This finding agrees with field observations of varying dielectric lens performance depending on orientation.

Results to date indicate that there is a residual air gap between specimen and cavity end wall of nearly 1 mil for all but the most conformable materials. Assuming a one mil gap for the TFE disks in lines 3 and 4 reduces the value of ϵ_{xy} to 2.09 in agreement with the double disk value. The tests with centrally located specimens were carried out with the bottom of the specimen flush with the lower lip of the top of the cavity. This results in specimens over 30 mils being increasingly off-center and slightly lowering their apparent ϵ_{xy}. The reduction of observed ϵ_{xy} due to a partial peripheral air gap should be less than $0.1\epsilon_{xy}\%$ if the disk diameter is at least 0.999 inch. Before machining the disks the copper should be etched off materials which shrink during etching.

Program

User Instructions: 1) load program, 2) key in specimen thickness, t, mils, press ENTER; 3) key in empty cavity resonant frequency f_0GHz, press ENTER, and 4) key in loaded cavity resonant frequency f_d, GHz, press A. Program first calculates and displays L (cm). For end specimen press R/S at this and next pause. For center located specimen press C at first pause, D at second.

STEP	KEYS	CODE	STEP	KEYS	CODE
1	LbL A	312511	70	√	3154
2	CL REG	3143	71	.	83
3	X^2	3254	72	2	02
4	STO A	3311	73	0	00
5	R ▼	3553	74	9	09
6	X^2	3254	75	6	06
7	STO B	3312	76	STO 9	3309
8	GSB b	322212	77	X	71
9	RTN	3522	78	π	3573
10	Lbl e	322515	79	X⇄Y	3552
11	X⇄Y	3552	80	÷	81
12	2	02	81	RTN	3522
13	.	83	82	Lbl C	312513
14	5	05	83	.	83
15	4	04	84	5	05
16	X	71	85	STO X9	337109
17	-	51	86	R ▼	3553
18	STO C	3313	87	GTO e	223115
19	LST X	3582	88	Lbl E	312515
20	STO D	3314	89	RCL 1	3401
21	÷	81	90	Pause	3572
22	RCL C	3413	91	RCL 9	3409
23	RCL 9	3409	92	÷	81
24	X	71	93	RCL D	3414
25	RCL A	3411	94	÷	81
26	RCL 8	3408	95	X^2	3254
27	-	51	96	RCL 8	3408
28		3154	97	+	61
29	X	71	98	RCLA	3411
30	RAD	3542	99	÷	81
31	GSB a	322211	100	RTN	3522
32	CHS	42	101	Lbl a	322511
33	X	71	102	TAN X	3164
34	RTN	3522	103	LST X	3582
35	1/X	3562	104	÷	81
36	1	01	105	RTN	3522
37	(-)	51	106	Lbl d	322514
38	CHS	42	107	TAN X	3164
39	STO 0	3300	108	LST X	3582
40	1	01	109	X	71
41	STO 1	3301	110	1/X	3562
42	Lbl B	312512	111	RTN	3522
43	DSP 6	2306	112	Lbl D	312514
44	RCL 1	3401	113	CHS	42
45	GSB a	322211	114	3	03
46	1/X	3562	115	1/X	3562
47	1	01	116	+	61
48	-	51	117	STO 0	3300
49	CHS	42	118	.	83
50	RCL 0	3400	119	1	01
51	X⇄Y	3552	120	STO 1	3301
52	÷	81	121	Lbl c	322513
53	√	3154	122	DSP 6	2306
54	Pause	3572	123	RCL 1	3401
55	STO X 1	337101	124	GSB d	322214
56	FRAC	3283	125	3	03
57	DSP 4	2304	126	1/X	3562
58	RND	3124	127	+	61
59	X = 0?	3151	128	RCL 0	3400
60	G 0 E	2215	129	÷	81
61	G 0 B	2212	130	√	3154
62	Lbl b	322512	131	Pause	3572
63	4	04	132	STO X 1	337101
64	7	07	133	FRAC	3283
65	.	83	134	DSP 4	2304
66	8	08	135	RND	3124
67	4	04	136	X = 0	3151
68	STO 8	3308	137	GTO E	2215
69	-	51	138	GSB c	322213

REFERENCES

1. N.G. Alexopoulos and O.M. Krowhe, IEEE Trans. MTT-26(6), 387-393 (June, 1978).
2. B.T. Szentkuti, Elec., Let 12 (25) 672-3 (9 Dec. 76)
3. R.P. Owens, J.E. Aitken and T.C. Edwards, IEEE MTT-24(8) 499-505 (Aug. 1976)
4. M. Kobayashi, IEEE Trans, MTT-26(2) 119-26 (Feb. 1978)
5. N.G. Alexopoulos and N.K. Uzunoglu, IEEE Trans. MTT-26 (6) 455-6 (June, 1978)
6. M. Kobayashi, IEEE Trans. MTT-26 (7), 510-12 (July, 1978)
7. B.T. Szentkuti, in ETHZ Report No. 77-09 (Eidgenossische Tech. Hoch schule Zurich (1977)
8. L.S. Napoli and J.J. Hughes, IEEE Trans. MTT-19 (7), 664-5 (July 1971)
9. T.J. Lynch COMSAT Memo TCLT/71-5084 (Dec. 1971)
10. M. Olyphant, IEEE trans. IM-20(4) 342-4 (Nov. 1971)
11. J. Deutsch and H.J. Jung NTZ-10, 463-4 (Oct. 1972)
12. H.F. Lenzing, Paper #41-E-72, Ann. Meeting, Am. Cer. Soc. May, 1972 (Washington, D.C.).
13. M. Olyphant, 1971 Ann. Report, Conf. on Elec. Insul. and Dielectric Phen. (Nat. Acad. of Sciences) 180-9 (1972)
14. J.G. Howell, IEPE Trans. MTT-21(31) 142-3 (March, 1973).
15. S. Ramo, J.R. Whinnery and T. Van Duzer, Fields and Waves in Communication Electronics (J. Wiley and Sons, New York, 1965).